Appl Microbiol Biotechnol (2017) 101:4923–4933
DOI 10.1007/s00253-017-8188-6

Sortase A-aided *Escherichia coli* expression system for functional osteoprotegerin cysteine-rich domain

Mengmeng Jin[1] · Yuan Chen[2] · Yunfeng Zhao[2] · Luyang Che[1] · Yanyan Ma[3] · Jingzhe Li[3] · Yi Wang[3] · Hua Tao[2] · Juan Ma[2] · Bing Pan[4] · Changzhen Liu[3] · Peng Huang[1]

Received: 12 November 2016 / Revised: 23 January 2017 / Accepted: 4 February 2017 / Published online: 16 March 2017

Abstract As a natural inhibitor of the receptor activator of nuclear factor-κB ligand (RANKL), osteprotegerin (OPG) is considered a promising treatment for metabolic bone diseases. Typical approaches for preparing recombinant OPG or its derivatives employ eukaryotic expression systems. Due to the advantages of a prokaryotic expression system, which include its convenience, low cost, and abundant production, in this study, we establish a strategy for preparing functional OPG using the *Escherichia coli* expression system. After initial failures in preparation of OPG and its truncation, OPG cysteine-rich domain (OPG-CRD/OPGT) by using pET and pGEX vectors, we constructed a sortase A (SrtA)-aided *E. coli* expression system, in which the expressed protein was a self-cleaving SrtA fusion protein. Using this system, we successfully prepared the recombinant OPGT protein. The BIAcore analyses indicated that the prepared OPGT had high affinities in binding with RANKL and TRAIL. Cell experiments confirmed the inhibitory effects of the prepared OPGT on RANKL-induced osteoclast differentiation and TRAIL-induced tumor cell apoptosis. The sortase A-aided *E. coli* expression system for OPGT established in this study may contribute to further studies and commercial applications of OPG.

Keywords OPG-CRD/OPGT · SrtA-aided *E. coli* expression system · RANKL · TRAIL

Mengmeng Jin and Yuan Chen contributed equally to this work.

✉ Changzhen Liu
lcz0220@163.com

✉ Peng Huang
harryhp@vip.sina.com

[1] The People's Liberation Army General Hospital, 28 Fuxing road, Beijing 100853, China

[2] CAS Key Laboratory of Pathogenic Microbiology and Immunology, Institute of Microbiology, Chinese Academy of Sciences, 1 Beichen Xilu, Beijing 100101, China

[3] Beijing Key Laboratory of Research of Chinese Medicine on Prevention and Treatment for Major Diseases, Experimental Research Center, China Academy of Chinese Medical Sciences, NO.16, Dongzhimennei South Street, Dongcheng District, Beijing 100700, China

[4] Beijing Jiquan Biology Technology Co., LTD, No.8 HaiYing Rd., Fengtai District, Beijing 100070, China

Introduction

Osteoprotegerin (OPG), also known as osteoclastogenesis inhibitory factor (OCIF) or tumor necrosis factor receptor superfamily member 11b (TNFRSF11B), is a member of the tumor necrosis factor receptor (TNFR) family (Simonet et al. 1997; Yamaguchi et al. 1998). In contrast to most TNFR family members which are transmembrane receptors with functional cytoplasmic domains, OPG is a soluble secreted protein. It consists of approximately 401 amino acids and there is ~85% identity between the mouse and human homologs. OPG has three major structural motifs: a four cysteine-rich TNF receptor domain (CRD) which is a characteristic motif among TNFR family members, a heparin-binding domain, and two death domain homologous regions (DDH), through which OPG is assembled as a homodimer (Yamaguchi et al. 1998).

There are two main known roles for OPG at the molecular level: inactivating the receptor activator of nuclear factor-κB ligand (RANKL) and the TNF-related apoptosis-inducing ligand (TRAIL) (Vitovski et al. 2007). As a decoy receptor, OPG binds to RANKL, whose functional receptor is the receptor activator of NF-κB (RANK), and inhibits the RANKL/

RANK pathway. Nowadays, the RANKL/RANK/OPG system is believed to be one of the most important signaling axes regulating bone metabolism (Boyce and Xing 2008; Sattler et al. 2004; Theill et al. 2002). Among the systems, the importance of OPG has been demonstrated in *OPG* knockout mice which exhibited severe osteoporosis (Bucay et al. 1998; Mizuno et al. 1998). It has also been demonstrated that the OPG/RANKL ratio represents an important determinant of bone resorption in several disease models (Kearns et al. 2008). Additionally, it has been suggested that the RANKL/RANK/OPG system is associated with vascular calcification (Collin-Osdoby 2004; D'Amelio et al. 2009). By binding to RANK and subsequently increasing BMP4 production via the activation of the alternative NF-κB pathway, RANKL induced the deposition of a mineralized matrix produced by vascular smooth muscle cells (Panizo et al. 2009). OPG appears to inhibit this process. It has been shown that *OPG* knockout mice developed calcified lesions in the aorta and renal arteries (Bucay et al. 1998; Orita et al. 2007), which suggests that OPG plays a protective role through its prevention of vascular calcification. OPG also acts as a decoy receptor for TRAIL and blocks the initiation of apoptosis (Lane et al. 2012). It used to be believed that TRAIL selectively induces cancer cell apoptosis and has no influence on normal organs or tissues (Walczak et al. 1999). However, researches indicated that TRAIL may also induce apoptosis of normal human hepatocytes, cultured human microvascular endothelial cells, and kidney cells (Jo et al. 2000; Montanez-Barragan et al. 2014; Pritzker et al. 2004). As the natural inhibitor of TRAIL, OPG obviously protects the normal organs or tissues from TRAIL cytotoxicity. Indeed, abnormal OPG/TRAIL ratios have been shown to be associated with severe acute myocardial infarction and the early onset of diabetes mellitus (Secchiero et al. 2010; Vaccarezza et al. 2007). In another aspect, several tumor cells including prostate cancer cells, multiple myeloma cells, breast cancer cells, and colorectal cancer cells are also protected from TRAIL-induced apoptosis by OPG, which secreted by osteoblast-like cells and bone marrow stromal cells, as well as cancer cells themselves (Corey et al. 2005; De Toni et al. 2008; Neville-Webbe et al. 2004; Rachner et al. 2009; Shipman and Croucher 2003).

Nowadays, treatment with RANKL inhibitors presents a promising strategy for the treatment of various disease settings, e.g., osteoporosis, rheumatoid arthritis, cancer metastasis, and other metabolic bone diseases (Delmas 2008; Wada et al. 2006). As a natural RANKL inhibitor, OPG is also considered as a possible treatment for such diseases. A phase I clinical trial has shown that AMGN-0007, a derivative of OPG, can be an effective treatment for multiple myeloma and breast carcinoma-related bone metastases (Body et al. 2003). Not all parts of OPG are needed for drug development. Studies have revealed that the CRD domain (22–201) of OPG (OPG-CRD/OPGT) is responsible for the binding of RANKL (Luan et al. 2012; Nelson et al. 2012; Simonet et al. 1997). The effectiveness of OPGT as a neutralizing agent against RANKL has been verified with AMGN-0007, which consists of the 22–194 region of OPG and a C-terminal immunoglobulin Fc fragment (Body et al. 2003).

Due to the therapeutic potential of OPG and its derivatives, it is valuable to investigate approaches for OPG or OPGT protein preparation. To date, the most common approaches employ eukaryotic expression systems, such as the CHO cell expression system (Body et al. 2003; Simonet et al. 1997), baculovirus-infected insect cells (Luan et al. 2012; Nelson et al. 2012), and the yeast expression system (He et al. 2000; LIU et al. 2009). Reports from Amgen Incorporation mentioned that Fc-OPG, an OPG derivative, was prepared from *Escherichia coli* (Bekker et al. 2001; Lacey et al. 2012; Morony et al. 1999). However, there has been no detailed description of their preparation procedure to our knowledge. In this study, we introduce a sortase A-aided *E. coli* expression system to produce the functional OPGT. This sortase A-aided *E. coli* expression system may contribute to the commercial applications of functional OPGT, due to its advantages of large-scale production and cost reduction, or it may contribute to scientific researches for its convenient use in protein preparations in further experiments related to multiple mutations or modifications of this protein.

Materials and methods

Construction of plasmids

The complementary DNA (cDNA) encoding SrtA was amplified using PCR from group A streptococci (GAS) M1 strain (90–226) (Fan et al. 2014). The DNA sequence encoding the LPETG peptide (LPETGGG) was introduced onto the 3′ end of the SrtA (accession number: NC002737) gene using the designed primer (Fan et al. 2014). The PCR products were cloned into the *Nco* I and *Sal* I site of the pET28a vector and the constructed vector was named pET28a-SrtA. The cDNA encoding full-length human OPG (accession number: U94332) was obtained using RT-PCR from the messenger RNA (mRNA) of human peripheral blood mononuclear cells. The full-length OPG and its truncation, a DNA sequence encoding OPGT (residues 22–201 of OPG, OPG-CRD), were then cloned into the *Nco* I and *Xho* I sites of the pET28a vector. The OPGT cDNA was also cloned into the *Bam*H I and *Sal* I sites of the pGEX-6p-1 vector, and the *Sal* I and *Xho* I sites of the constructed pET28a-SrtA vector. The proteins produced from these constructed vectors were OPG/OPGT, GST-OPGT fusion protein, and SrtA-LPETG-OPGT fusion protein. The cDNA encoding the truncation of human TRAIL (residues 115–281 of TRAIL, soluble TRAIL, sTRAIL) was obtained using RT-PCR from the mRNA of

human peripheral blood mononuclear cells and cloned into the *Bam*H I and *Sal* I sites of the pGEX-6p-1 vector. The expressed plasmid for GST-RANKL (encoding residues 159–361 of human RANKL) and RANK (encoding residues 159–361 of human RANK) were prepared previously (Liu et al. 2015; Zhang et al. 2009). All constructed plasmids were confirmed by DNA sequencing.

Expression and purification of proteins

All recombinant proteins were expressed in the *E. coli* strain BL21(DE3). Bacteria with the constructed pGEX-6p-1 vectors were cultured in LB medium containing 100 μg/ml ampicillin at 37 °C under constant agitation (200 rpm). When an OD600 of 0.4 was attained, isopropyl β-d-1-thiogalactopyranoside (IPTG) was added to a final concentration of 0.5 mM for TRAIL expression or 0.1 mM for RANKL and OPGT expression. The cultures were then agitated at 150 rpm for an additional 5 h at 25 °C for TRAIL expression or overnight at 20 °C for RANKL and OPGT expression. The cells from 2 l of LB medium were harvested by centrifugation and lysed with a lysis buffer (50 mM Tris–HCl, 150 mM NaCl, 1 mM EDTA, 1 mM DDT, 1 mM lysozyme, 0.5% *v*/*v* Triton X-100, pH 8.0) by an ultrasonic cell crusher (Scientz Biotech, Ningbo, China) at a condition of 300 W, 3 s on and 5 s off, total time 23 min. The GST fusion proteins in the supernatant of the lysate were purified using affinity chromatography with Glutathione-Sepharose Fast Flow 4B beads (5 ml of beads for supernatant from 2 l of bacteria culture) according to the manufacturer's instructions (GE Healthcare). The GST tags were cleaved overnight at 4 °C using the PreScission protease (PSP, GE Healthcare, 20 μg for GST fusion protein prepared from 2 l of bacteria culture) and the proteins were further purified using size-exclusion chromatography (Superdex 200, GE Healthcare) in 0.1 M Tris pH 7.0 and 50 mM NaCl.

Bacteria with the constructed pET28 vectors were cultured in LB medium containing 100 μg/ml kanamycin, at 37 °C under constant agitation (200 rpm). For the expression of all proteins (RANK, OPG, OPGT, and SrtA-OPGT), IPTG was added to a final concentration of 1 mM for an additional 5 h at 37 °C when OD600 of 0.6 was attained. The cells were harvested by centrifugation and the pellet was re-suspended in 100-ml ice-cold washing buffer (50 mM Tris, 150 mM NaCl, 5 mM EDTA, 1% *v*/*v* Triton X-100, pH 8.0), and then disrupted and homogenized by sonication for 10 min (3 s on, 5 s off) using an Ultrasonic Cell Crusher and washed extensively with washing buffer. After repeated sonication and centrifugation, the inclusion bodies were dissolved at room temperature in 6 M guanidine hydrochloride, 50 mM Tris pH 8.5, 1 mM EDTA, 150 mM NaCl, and 10 mM DTT to produce a final protein concentration of 30 mg/ml (wet weight of the inclusion bodies). The refolding of recombinant proteins was performed by further dilution with 20 mM Na_2HPO_4 pH 7.3, 1 M L-arginine, 20% glycerol, 10 mM reduced glutathione, and 1 mM oxidized glutathione to a concentration of 10 mg/ml, followed by dialysis against 20 mM Na_2HPO_4 pH 7.3, 0.5 M L-arginine, and 10% glycerol for 12 h at 4 °C. Additional dialyses against 20 mM Na_2HPO_4 pH 7.3, 0.2 M L-arginine and 5% glycerol for 12 h at 4 °C were followed by two dialysis steps against 20 mM Na_2HPO_4 pH 7.3 for 12 h at 4 °C. After centrifugation at 20,000*g* for 10 min, the supernatant was collected and the refolded OPGT proteins, which with a designed His-tag on the C-terminus of OPGT, were further purified by the Ni-NTA affinity chromatography according to the manufacturer's instructions (GE Healthcare). Briefly, the supernatant diluted in 100 ml of the purification buffer (50 mM NaH_2PO_4, pH 8.0, 0.5 M NaCl) was mixed with the 5 ml of Ni-NTA affinity resins for 1 h at 4 °C under constant agitation (30 rpm). The resins were then collected by low-speed centrifugation (800*g*) for 5 min and washed with 20 ml of the purification buffer with 20 mM imidazole. After repeated centrifugation and washing of resins for three times, the binding proteins were then eluted by 20 ml of the purification buffer with 200 mM imidazole. After concentration by ultrafiltration, the eluted proteins were further purified using size-exclusion chromatography (Superdex 200, GE Healthcare) at the flow rate of 0.5 ml/min in 0.1 M Tris pH 7.0 and 50 mM NaCl.

MALDI-TOF mass spectrometer

MALDI-TOF mass spectrometer was used to characterize the sample prepared by the size-exclusion chromatography. In our study, MALDI analysis was performed on a Bruker Autoflex time-of-flight mass spectrometer. The instrument was equipped with a delayed ion-extraction device and a pulsed nitrogen laser operated at 337 nm, and its available accelerating potential was in the range of 20 kV. The MALDI uses a ground-steel sample target with 384 spots. The range of laser energy was adjusted to slightly above the threshold in order to obtain good resolution and good signal-to-noise ratio. Sinapinic acid (SA) was used as the matrix for MALDI analysis. We obtained the mass spectra reported in the positive-ion linear mode with delayed extraction for 50 ns and external mass calibration by using two points that bracketed the mass range of interest. Each mass spectrum was typically summed with 50 laser shots.

Surface plasmon resonance

The binding affinities of OPGT to RANKL and TRAIL were determined by surface plasmon resonance (SPR) using BIAcore 3000 at 25 °C. The RANKL or TRAIL was immobilized to ~2000 response units on one channel of a CM5 sensor chip in 10 mM sodium acetate, pH 5.5 using

the standard amine coupling method (Kim et al. 2003). Recombinant TNFRSF9 was immobilized on another channel as a reference. Different concentrations of OPGT (0, 3.125, 6.25, 12.5, 25, 50, and 100 nM) in 10 mM HEPES, 150 mM NaCl, 0.005% Tween 20, pH 7.4 were injected into both channels and the signals were recorded as sensorgrams. Sensorgrams were fitted into the 1:1 binding model using BIA evaluation software 4.1 (Biacore, GE Healthcare), and the equilibrium-dissociation constants (KD) were calculated.

Osteoclast differentiation assay

The osteoclast differentiation assay was performed according to methods we reported previously (Liu et al. 2010). Briefly, the murine monocytic cell line RAW264.7 was cultured in 24-well plates (1×10^4 cells/well) and maintained in α-MEM containing 10% (*v*/*v*) FBS. Then, 50 ng/ml of RANKL was added to the cell cultures to induce the differentiation of RAW264.7 cells into osteoclasts. Varying concentrations of OPGT were added to inhibit the RANKL-induced differentiation effect. After 4 days, the cells were fixed and stained using the Acid Phosphatase, Leukocyte (TRAP) Kit (Sigma-Aldrich, 387A) according to the manufacturer's instructions. The TRAP-positive, multinucleated (>3 cells per well) cells were counted under a light microscope using methods described previously (Polek et al. 2003). Aliquots of cells were used to quantify TRAP activity using methods described previously (Zhao et al. 2013). Briefly, the cells were washed once with PBS and lysed in 100 μl of cold lysis buffer (90 mM citrate buffer, pH 4.8, 0.1% Triton X-100 containing 80 mM sodium tartrate) for 10 min. After lysis, 100 μl of substrate solution (20 mM *p*-nitrophenyl phosphate in the above lysis buffer) was added and incubated for an additional 5 min. The reaction was terminated by adding 40 μl of 0.5 M NaOH. The optical density was read at a wavelength of 405 nm. Each experiment was repeated four times for statistical analysis.

Apoptosis assays

TRAIL-mediated apoptosis was assessed using sub-G1 DNA content analysis with a slight modification (Allen et al. 2012). Briefly, colo205 cells were exposed to 100 ng/ml of sTRAIL and varying concentrations of OPGT for 3 h. Cells were harvested, washed, re-suspended with phosphate-buffered saline (PBS pH 7.4) and fixed in 80% ethanol on ice. After being washed with PBS and re-suspended with PBS containing 0.2% Triton X-100 and 0.5 mg/ml of RNase A, cells were stained with 25 μg/ml propidium iodide and then subjected to analytic flow cytometry using a FACSort (BD Biosciences, Mountain View, CA).

Results

Expression of OPG using pET28a and pGEX-6p-1 expression system

For the preparation of functional OPG, we first expressed the full-length OPG, which fused with a C-terminal His-tag for affinity purification by NTA chromatography, using the *E. coli* strain BL21(DE3) containing the constructed pET28a-OPG vector (Fig. 1a). The results showed that although the RANK protein which was used as a positive control for the expression system was quite well expressed, there was no obvious expression of OPG protein (Fig. 1c). We were also unable to obtain any soluble OPG protein after purification from cell lysate using NTA affinity chromatography and the inclusion body amount was insufficient for next-step purification (data not shown). Because the CRD domain (22–201) of OPG (OPG-CRD, OPGT) was reported to be sufficient in binding and neutralizing RANKL (Luan et al. 2012; Nelson et al. 2012; Simonet et al. 1997), we then tried to prepare OPGT (OPG-CRD) instead of full-length OPG using the *E. coli* expression system. First, the *OPGT* sequence was inserted into the pET-28a vector (Fig. 1b). The results showed that there was still no obvious expression of the OPGT protein (Fig. 1c), and still no soluble OPGT protein and almost no inclusion body obtained. The *OPGT* sequence was then inserted into the pGEX-6P vector, in which a *GST* sequence was linked to the upstream region of the *OPGT* sequence (Fig. 1d). The fusion protein, GST-OPGT, was successfully expressed in BL21(DE3) by the induction of IPTG (Fig. 1e). However, we were still unable to obtain soluble OPGT protein after the GST agarose purification and the following PSP proteolytic cleavage (lane of purified GST-OPGT, Fig. 1f). SDS-PAGE analysis revealed that the expressed GST-OPGT mainly existed as inclusion bodies in the precipitate (lane of precipitation of lysate, Fig. 1f).

Expression and purification of OPGT using SrtA system

Although an abundant amount of GST-OPGT was found in the precipitate, due to the difficulty in refolding GST fusion protein, we abandoned the attempt to denature and refold the GST-OPGT protein. However, the largely increased production of OPGT by fusion with a GST moiety raised the possibility that the addition of N-terminal polypeptides may increase the expression of OPG proteins greatly. We then constructed a pET28a-SrtA-OPGT plasmid to prepare OPGT protein (Fig. 2a). Sortase A (SrtA) has been widely used as an in vitro tool to cleave or post-translationally modify engineered proteins. It selectively recognizes a LPXTG motif and cleaves in between the threonine and glycine (Navarre and Schneewind 1994). When a target protein is linked to its c-terminus by a LPXTG motif, it can cleave the linker region

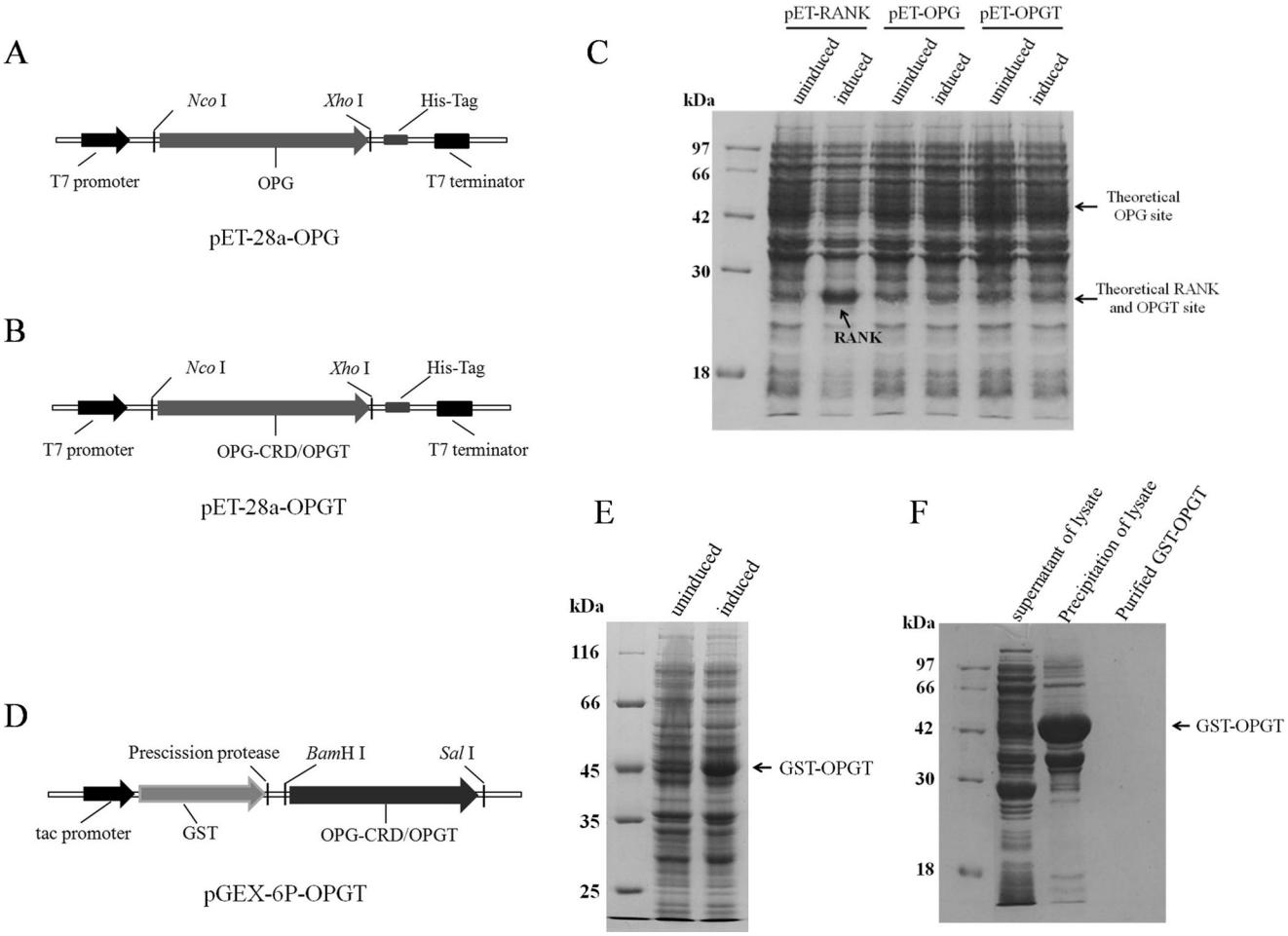

Fig. 1 Expression of OPG or OPGT using the pET-28a and pGEX-6p vector. **a**, **b** Schematic gene structure of constructed pET-28a-OPG and pET-28a-OPGT. **c** Expression of OPG and OPGT using the constructed pET-28a vector. Protein expression was induced with IPTG and cells were loaded onto 12% SDS-PAGE gel for analysis. The pET-28a-RANK was used as a positive control. **d** Schematic gene structure of the constructed pGEX-6p-OPGT. **e** Expression of GST-OPGT using the constructed pGEX-6p-OPGT vector. Protein expression was induced with IPTG at 20 °C and cells were loaded onto 12% SDS-PAGE gel for analysis. **f** SDS-PAGE analysis of the purified GST-OPGT fusion protein. After ultrasonication, centrifugation, and purification by affinity chromatography, the supernatant and precipitation of the lysate and the purified GST-OPGT fusion protein were analyzed by SDS-PAGE

and release the target protein. In the constructed pET28a-SrtA-OPGT vector, a SrtA gene sequence and a DNA sequence of the LPETG linker (LPETGGG) were linked to upstream of the *OPGT* gene sequence. After IPTG-induced expression and subsequent cell lysis, the expressed protein was found as an inclusion body in the insoluble portion of the lysate. The result from the SDS-PAGE analysis showed that based on the molecular weight (the theoretical molecular weight of SrtA-OPGT is 41.250 kD, while the OPGT without SrtA is 21.880 kD), the expressed protein in inclusion body was mainly composed of OPGT that was separated from SrtA via the self-cleavage of the SrtA fusion protein during protein expression (Fig. 2b). After the dissolution of the inclusion bodies and refolding, the refolded protein was purified using size-exclusion chromatography with the collection of the 15.11-ml peak (Fig. 2c). The result of the SDS-PAGE analysis confirmed the existence and purity of the desired OPGT (Fig. 2d). The precise molecular weight of the prepared protein (21.888 kD) measured by the MALDI-TOF mass spectrometer confirmed the integrity of the desired OPGT, whose molecular weight is 21.880 kD (Fig. 2e). Using this expression system, the yield of purified recombinant OPGT was approximately 10 mg per liter of LB medium in our laboratory.

High affinities of OPGT in binding with RANKL and TRAIL

The affinity between OPGT and RANKL (or TRAIL) is an important index at the molecular level to evaluate the inhibition ability of OPGT to its targeted protein. A very effective method for detecting the affinity between molecules is surface plasmon resonance (SPR) (Nguyen et al. 2015). In this study, the affinity of the prepared OPGT to RANKL or TRAIL was

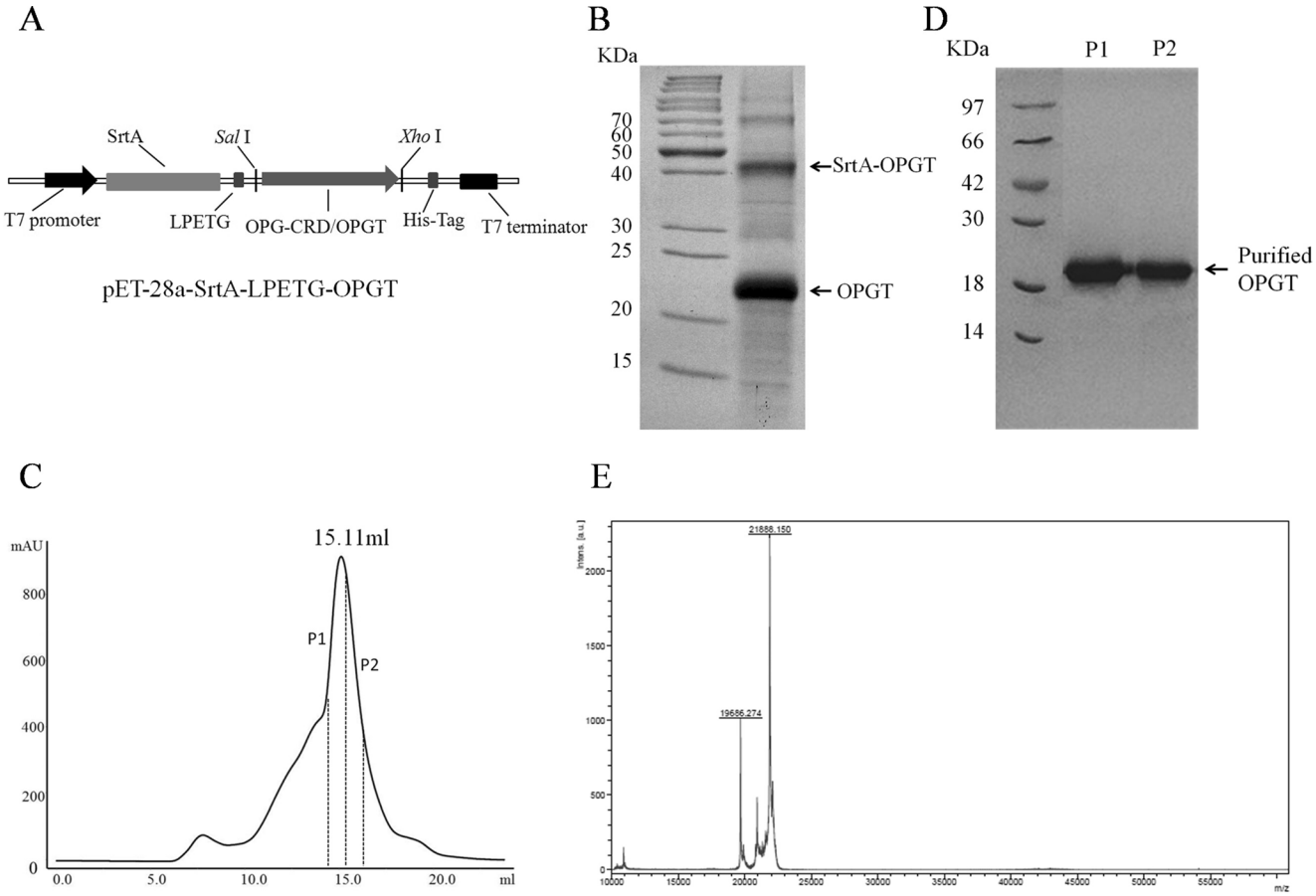

Fig. 2 Expression and purification of OPGT using the pET-28a-SrtA vector. **a** Schematic gene structure of the constructed pET-28a-SrtA-LPETG-OPGT. **b** Analysis of the inclusion bodies by the SDS-PAGE gel. The cells were crushed by sonication and washed extensively with washing buffer. After centrifugation, the pellet was loaded onto 12% SDS-PAGE gel for analysis. **c** Purification of the refolded proteins using the size-exclusion chromatography. The inclusion bodies were dissolved in guanidine hydrochloride solution and dialyzed against the dialysis buffer. The refolded proteins were subjected to the size-exclusion chromatography (Superdex 200, GE Healthcare). **d** Identification of the purified OPGT. The two components collected from 14.50 to 15.20 ml (*P1*), and 15.20 to 15.90 ml (*P2*) of the size-exclusion chromatography were analyzed by 12% SDS-PAGE. **e** The precise molecular weight of the purified OPGT was determined by the MALDI-TOF mass spectrometer

measured using Biacore 3000, a highly sensitive SPR detecting system. RANKL and TRAIL were immobilized in different channels on a CM5 sensor chip. Recombinant TNFRSF9, a nonspecific protein control, was immobilized in another channel on the same chip. Different concentrations of OPGT were passed through the chip one at a time to record the interaction signals. As seen in Fig. 3, the average KD of OPGT for TRAIL was 4.39×10^{-9} M (Fig. 3a) and for RANKL was 1.19×10^{-9} M (Fig.3b).

E. coli purified OPGT could inhibit the differentiation of RAW264.7 into osteoclast

The differentiation assay of the murine monocytic cell line RAW264.7 into osteoclast was carried out to assess the ability of the prepared OPGT to inhibit RANKL-induced differentiation. Osteoclast differentiation and maturation induced by osteotropic factors including RANKL is characterized by the formation of giant multinucleated cells (MNCs) and the expression of tartrate-resistant acidic phosphatase (TRAP) in MNCs (Filgueira 2004; Simonet et al. 1997). The number of TRAP-positive MNCs and the level of TRAP activity, which usually are detected using histochemical methods for light microscopy or spectroscopy are used to estimate the degree of osteoclast differentiation and maturation (Miyamoto 2011; Simonet et al. 1997). In this study, as shown in Fig. 4a, b, there were no TRAP-positive cells or mature osteoclasts (TRAP-positive, multinuclear cells with diameter >100 μm) in the control group, which contained neither of the proteins. In the RANKL alone group, the human-derived RANKL used in this study successfully induced the formation of TRAP-positive cells and mature osteoclasts due to evolutionary conservation of RANKL protein. Accompanying the increase of molar ratio of OPGT to RANKL, less TRAP-positive cells were observed. The numbers of mature osteoclasts decreased and approached zero when the molar ratio of OPGT to RANKL was 5:1 or more. Using spectroscopic measurement with a wavelength of 405 nm, we further assessed the TRAP activity

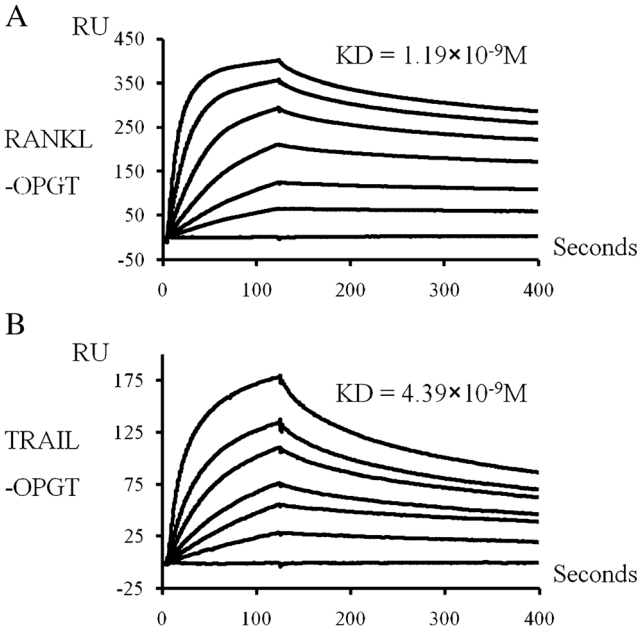

Fig. 3 The affinities of OPGT to TRAIL and RANKL. The affinities of TRAIL and hRANKL for binding to OPGT were measured by BIAcore analyses using a chelating CM5 sensor chip. Recombinant TNFRSF9 was used as a negative control. Varying concentrations of OPGT (0, 3.125, 6.25, 12.5, 25, 50, and 100 nM) were injected into channels and the signals were recorded as sensorgrams. The equilibrium-dissociation constants were calculated using BIAevaluation software 4.1

of the RAW264.7 cells cultured with RANKL and different concentrations of OPGT. The results showed that with increased concentrations of OPGT, the TRAP activity decreased (Fig. 4c). These results indicated that the prepared OPGT could inhibit RANKL-induced osteoclast differentiation.

E. coli purified OPGT could inhibit the TRAIL-induced apoptosis

We then used sub-G1 DNA content analysis to measure the inhibitory effects of the prepared OPGT on TRAIL-mediated colo205 cell apoptosis. Colo205 cells are highly sensitive to TRAIL and therefore are used widely in detections of TRAIL-induced apoptosis (Lippa et al. 2007). The sub-G1 DNA content analysis is also the classical method for measuring the modulation effects of agents on TRAIL-induced apoptosis (Nakata et al. 2004). As shown in Fig. 5a, b, after treating the colo205 cells with 100 ng/ml TRAIL for 3 h, the percentage of sub-G1 phase cells increased from approximately 5 to 40%. Relative to the treatment with TRAIL alone, the co-treatment of cells with TRAIL and different concentrations of OPGT resulted in decreased amounts of sub-G1 phase cells. This decrease was in a OPGT dose-dependent manner, thus indicating the inhibitory effects of the prepared OPGT on TRAIL.

Discussion

OPG was discovered unexpectedly by researchers at Amgen in studies designed to find novel tumor necrosis factor receptor (TNFR)-related molecules that could interfere with TNF signaling (Boyce and Xing 2008). RANKL promotes osteoclast development through RANK activation, while OPG inhibits this process by competitively binding to RANKL. Its antagonistic activity makes this naturally occurring RANKL inhibitor a promising therapeutic candidate for the treatment of disorders related to the abnormal expression of RANKL.

Reports from Amgen Incorporation mentioned that Fc-OPG was prepared from *E. coli* (Bekker et al. 2001; Lacey et al. 2012; Morony et al. 1999); however, there has been no detailed description of their preparation procedure to our knowledge. On the contrary, almost all published reports employ eukaryotic expression systems in the preparations of OPG or its derivative. In 1997, Simonet WS et al. expressed human and mouse OPG using 293E and CHO cells (Simonet et al. 1997). Preparations of recombinant OPG from the pichia pastoris yeast strain, HEK293 cell, or COS-7 cell have also been reported in the following studies (Cundy et al. 2002; Emery et al. 1998; He et al. 2000; LIU et al. 2009; Truneh et al. 2000). In 2012, two research groups expressed OPG using baculovirus-infected insect cells and solved the structure of RANKL/OPG individually (Luan et al. 2012; Nelson et al. 2012). AMGN-0007, an alternative recombinant OPG-Fc developed by Amgen Incorporation in order to improve the half-life through the glycosylation of the Fc region, was also prepared using CHO cells (Body et al. 2003). Thus, in this study, we aimed to prepare OPG using the *E. coli* expression system. At the beginning stage, we used pET and pGEX vectors, which are the most common vectors used in the *E. coli* expression system, to express OPG and its truncation, OPGT. There was no obvious OPG or OPGT expression in bacteria with the pET28 vector. An abundant amount of GST-OPGT protein appeared in bacteria with the pGEX-6P vector. However, the expressed GST-OPGT existed mainly as inclusion bodies, and little soluble protein was obtained. This phenomenon indicated a possibility that it is difficult to express OPG or OPGT alone using the *E. coli* expression system for unknown reasons, and this possibility may account for why OPG and its derivative were rarely prepared using *E. coli* expression systems in the reports. The high yield produced using the pGEX-6P vector also suggested that the addition of an N-terminal polypeptide which is easier to express may contribute greatly to the expression of fused OPG proteins. Correspondingly, the OPG derivative Fc-OPG developed by the Amgen Incorporation using *E. coli* is this form of fusion protein (Morony et al. 1999).

Based on our supposition, we chose SrtA as the N-terminal fused polypeptide. SrtA is a type of transpeptidase produced by gram-positive bacteria such as *Staphylococcus aureus*

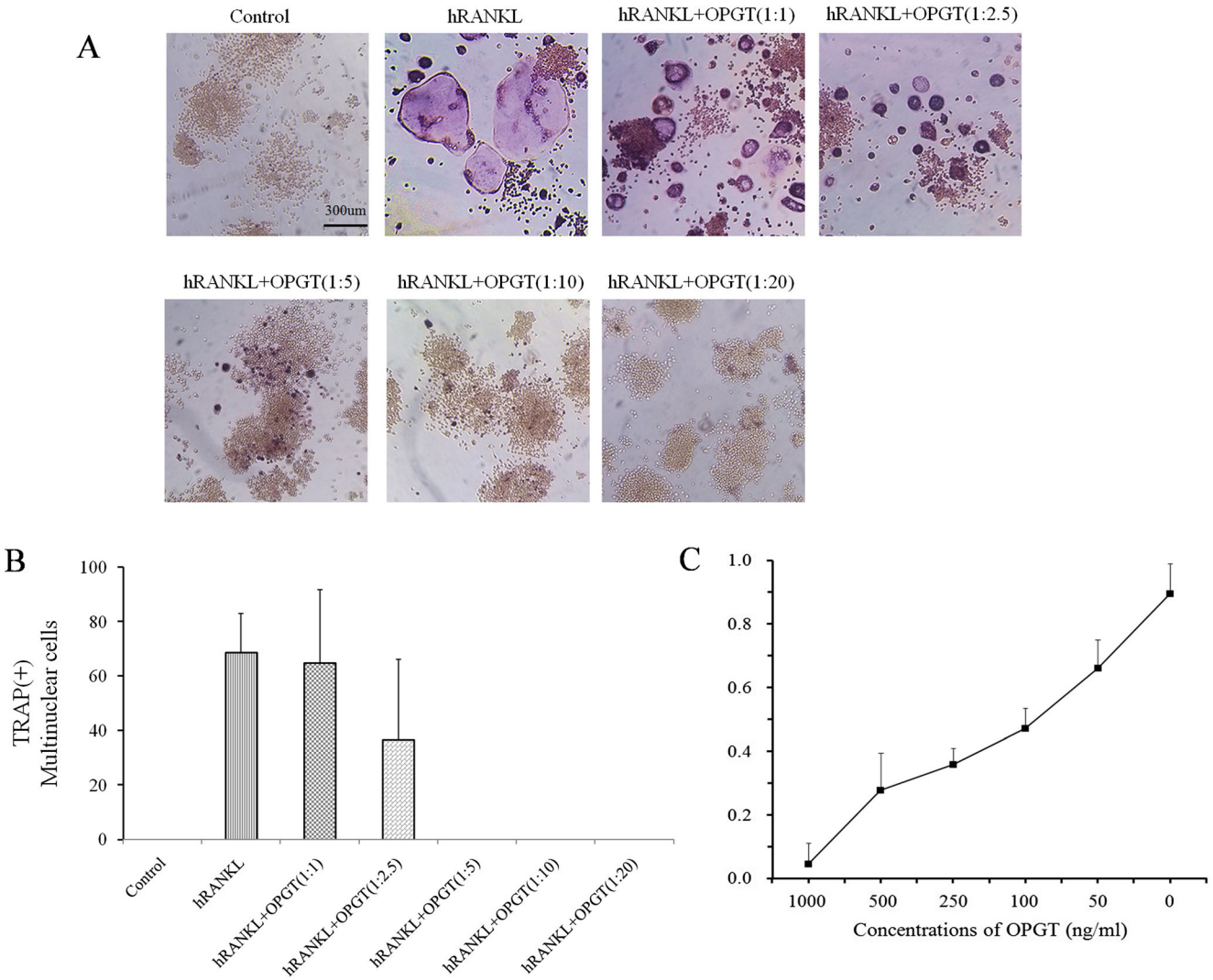

Fig. 4 The inhibition of osteoclastogenesis mediated by OPGT. **a** Different ratios of RANKL and OPGT were added to the RAW264.7 cell cultures. The concentration of hRANKL was 50 ng/ml and the concentrations of OPGT were 50, 125, 250, 500, and 1000 ng/ml. RAW264.7 cells without RANKL and OPGT served as the control. *Scale bar*, 300 μm. **b** The multinucleated, TRAP staining-positive, and large diameter (>100 μm) cells were counted. The *bar* represents the average of four independent experiments; the data are shown as the mean ± SD. **d** TRAP activity of the RAW264.7 cells cultured with RANKL and different concentrations of OPGT. All groups were cultured in α-MEM medium containing 50 ng/ml of RANKL. The *curve* represents the average of four independent experiments with SD bars

(Cossart and Jonquieres 2000). It recognizes and specially cleaves the short recognition motif (LPXTG) on the target protein and has been widely used as an in vitro tool to cleave or post-translationally modify engineered proteins. In this study, we adopted one of its recognition sequences, LPETG, to link SrtA and OPGT to separate SrtA from OPGT through the self-cleavage of the fusion protein. The results showed that we successfully obtained an abundance of cleaved OPGT inclusion bodies. After denaturing, refolding, and purification, we obtained the soluble form of OPGT. It was reported that calcium ions (2 mM or more concentrations) are required for efficient SrtA catalysis (Ilangovan et al. 2001). However, in this study, although no additional calcium ion was added, the self-cleavage of SrtA fusion protein was nearly completed based on the result from Fig. 2b, indicating that the inherent calcium ions in the *E. coli* expression system may be sufficient for the self-cleavage of SrtA-OPGT fusion protein. This supposition is not in conflict with the previous report since there is still some activity of SrtA when incubating in a calcium-free buffer (Ilangovan et al. 2001). Whether the addition of calcium ions promotes the efficiency of self-cleavage or the product yield of OPGT will be investigated in future research.

Subsequently, the Biacore analyses showed that the affinity constants between OPGT and RANKL, and between OPGT and TRAIL were 1.19×10 and 4.39×10^{-9} M, respectively. In the previous reports using the baculovirus-infected insect system, the affinity constants of two types of OPG-CRD/OPGT (residues 22 to 186 and residues 22 to 197 of OPG) to

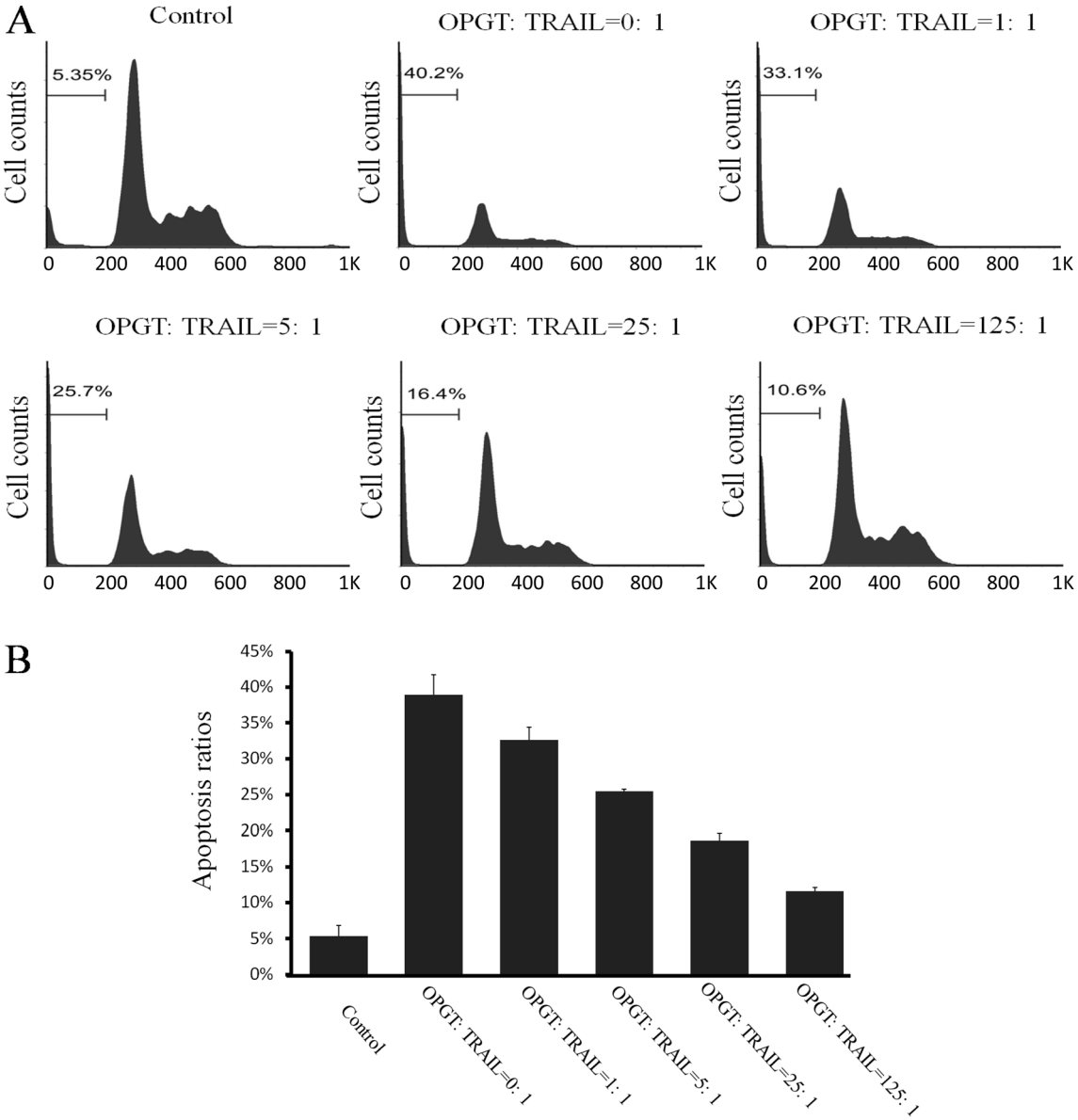

Fig. 5 Flow cytometric analysis of apoptotic cells. Colo205 cells were treated with sTRAIL (100 ng/ml) in either the absence or the presence of OPGT (molar ratios of OPGT to sTRAIL varying from 1:1 to 125:1) for 3 h. Apoptosis was analyzed as a sub-G1 fraction by fluorescence-activated cell sorting. **b** The percentages of the sub-G1 fraction were calculated. The *bar* represents the average of three independent experiments; the data are shown as the mean ± SD

RANKL were 6.5×10^{-10} M and $5.14 \pm 2.99 \times 10^{-9}$ M, respectively (Luan et al. 2012; Nelson et al. 2012). Therefore, the OPGT prepared in this study has a similar binding affinity for RANKL as those reported previously using the baculovirus-infected insect system. There are no reports on the affinity constant between OPGT and TRAIL. One report mentioned that the affinity constant between TRAIL and OPG-Fc (the bivalent form of OPG by fusion to the Fc domain) prepared from CHO cells is 3×10^{-9} M (Emery et al. 1998). Therefore, in light of typically enhanced effect of the fused Fc domain on the ligand-receptor binding, the affinity of OPGT prepared using *E. coli* expression systems in this study for TRAIL should be as strong as the affinity of those prepared from CHO cells. Subsequent cell experiments also confirmed the inhibitory effects of OPGT on RANKL-induced osteoclast differentiation and TRAIL-induced tumor cell apoptosis.

In summary, we successfully constructed an SrtA-aided *E. coli* expression system for preparing OPGT, a functional truncation of OPG. The prepared OPGT possessed a high affinity for RANKL and TRAIL, and similar to the wild-type OPG, it effectively blocked RANKL-induced osteoclast differentiation and TRAIL-induced tumor cell apoptosis. This study

may provide valuable contribution to further studies investigating OPG mutations and modifications and may potentially benefit the commercial application of this protein.

Acknowledgements This work was supported by grants from the National Natural Science Foundation of China (grant no. 31170829, 31400754, 81171762, 81550017, and 81373884) and Beijing New-star Plan of Science and Technology (grant no. 2007B059), China & Croatia inter-governmental cooperation (grant no. 7-10).

Compliance with ethical standards This article does not contain any studies with human participants or animals performed by any of the authors.

Conflict of interest The authors declare that they have no conflict of interest.

References

Allen JE, Ferrini R, Dicker DT, Batzer G, Chen E, Oltean DI, Lin B, Renshaw MW, Kretz-Rommel A, El-Deiry WS (2012) Targeting TRAIL death receptor 4 with trivalent DR4 Atrimer complexes. Mol Cancer Ther 11(10):2087–2095. doi:10.1158/1535-7163.MCT-12-0366

Bekker PJ, Holloway D, Nakanishi A, Arrighi M, Leese PT, Dunstan CR (2001) The effect of a single dose of osteoprotegerin in postmenopausal women. J Bone Miner Res 16(2):348–360. doi:10.1359/jbmr.2001.16.2.348

Body JJ, Greipp P, Coleman RE, Facon T, Geurs F, Fermand JP, Harousseau JL, Lipton A, Mariette X, Williams CD, Nakanishi A, Holloway D, Martin SW, Dunstan CR, Bekker PJ (2003) A phase I study of AMGN-0007, a recombinant osteoprotegerin construct, in patients with multiple myeloma or breast carcinoma related bone metastases. Cancer 97(3 Suppl):887–892. doi:10.1002/cncr.11138

Boyce BF, Xing L (2008) Functions of RANKL/RANK/OPG in bone modeling and remodeling. Arch Biochem Biophys 473(2):139–146. doi:10.1016/j.abb.2008.03.018

Bucay N, Sarosi I, Dunstan CR, Morony S, Tarpley J, Capparelli C, Scully S, Tan HL, Xu W, Lacey DL, Boyle WJ, Simonet WS (1998) Osteoprotegerin-deficient mice develop early onset osteoporosis and arterial calcification. Genes Dev 12(9):1260–1268

Collin-Osdoby P (2004) Regulation of vascular calcification by osteoclast regulatory factors RANKL and osteoprotegerin. Circ Res 95(11):1046–1057. doi:10.1161/01.RES.0000149165.99974.12

Corey E, Brown LG, Kiefer JA, Quinn JE, Pitts TE, Blair JM, Vessella RL (2005) Osteoprotegerin in prostate cancer bone metastasis. Cancer Res 65(5):1710–1718. doi:10.1158/0008-5472.CAN-04-2033

Cossart P, Jonquieres R (2000) Sortase, a universal target for therapeutic agents against gram-positive bacteria? Proc Natl Acad Sci U S A 97(10):5013–5015

Cundy T, Hegde M, Naot D, Chong B, King A, Wallace R, Mulley J, Love DR, Seidel J, Fawkner M, Banovic T, Callon KE, Grey AB, Reid IR, Middleton-Hardie CA, Cornish J (2002) A mutation in the gene TNFRSF11B encoding osteoprotegerin causes an idiopathic hyperphosphatasia phenotype. Hum Mol Genet 11(18):2119–2127

D'Amelio P, Isaia G, Isaia GC (2009) The osteoprotegerin/RANK/RANKL system: a bone key to vascular disease. J Endocrinol Investig 32(4 Suppl):6–9

De Toni EN, Thieme SE, Herbst A, Behrens A, Stieber P, Jung A, Blum H, Goke B, Kolligs FT (2008) OPG is regulated by beta-catenin and mediates resistance to TRAIL-induced apoptosis in colon cancer. Clin Cancer Res 14(15):4713–4718. doi:10.1158/1078-0432.CCR-07-5019

Delmas PD (2008) Clinical potential of RANKL inhibition for the management of postmenopausal osteoporosis and other metabolic bone diseases. J Clin Densitom 11(2):325–338. doi:10.1016/j.jocd.2008.02.002

Emery JG, McDonnell P, Burke MB, Deen KC, Lyn S, Silverman C, Dul E, Appelbaum ER, Eichman C, DiPrinzio R, Dodds RA, James IE, Rosenberg M, Lee JC, Young PR (1998) Osteoprotegerin is a receptor for the cytotoxic ligand TRAIL. J Biol Chem 273(23):14363–14367

Fan X, Wang X, Li N, Cui H, Hou B, Gao B, Cleary PP, Wang B (2014) Sortase A induces Th17-mediated and antibody-independent immunity to heterologous serotypes of group A streptococci. PLoS One 9(9):e107638. doi:10.1371/journal.pone.0107638

Filgueira L (2004) Fluorescence-based staining for tartrate-resistant acidic phosphatase (TRAP) in osteoclasts combined with other fluorescent dyes and protocols. J Histochem Cytochem 52(3):411–414

He Z-Y, Yang G-Z, Chen Z-Y, Li B, Zhang W-J, Wu X-F (2000) A novel isoform of osteoprotegerin gene: cloning and expression and its hypocalcemic effect in mice. Protein and Peptide Letters 7(4):233–240

Ilangovan U, Ton-That H, Iwahara J, Schneewind O, Clubb RT (2001) Structure of sortase, the transpeptidase that anchors proteins to the cell wall of *Staphylococcus aureus*. Proc Natl Acad Sci U S A 98(11):6056–6061. doi:10.1073/pnas.101064198

Jo M, Kim TH, Seol DW, Esplen JE, Dorko K, Billiar TR, Strom SC (2000) Apoptosis induced in normal human hepatocytes by tumor necrosis factor-related apoptosis-inducing ligand. Nat Med 6(5):564–567. doi:10.1038/75045

Kearns AE, Khosla S, Kostenuik PJ (2008) Receptor activator of nuclear factor kappaB ligand and osteoprotegerin regulation of bone remodeling in health and disease. Endocr Rev 29(2):155–192. doi:10.1210/er.2007-0014

Kim JY, Lee MH, Jung KI, Na HY, Cha HS, Ko EM, Kim TJ (2003) Detection of antibodies against glucose 6-phosphate isomerase in synovial fluid of rheumatoid arthritis using surface plasmon resonance (BIAcore). Exp Mol Med 35(4):310–316. doi:10.1038/emm.2003.42

Lacey DL, Boyle WJ, Simonet WS, Kostenuik PJ, Dougall WC, Sullivan JK, San Martin J, Dansey R (2012) Bench to bedside: elucidation of the OPG-RANK-RANKL pathway and the development of denosumab. Nat Rev Drug Discov 11(5):401–419. doi:10.1038/nrd3705

Lane D, Matte I, Rancourt C, Piche A (2012) Osteoprotegerin (OPG) protects ovarian cancer cells from TRAIL-induced apoptosis but does not contribute to malignant ascites-mediated attenuation of TRAIL-induced apoptosis. J Ovarian Res 5(1):34. doi:10.1186/1757-2215-5-34

Lippa MS, Strockbine LD, Le TT, Branstetter DG, Strathdee CA, Holland PM (2007) Expression of anti-apoptotic factors modulates Apo2L/TRAIL resistance in colon carcinoma cells. Apoptosis 12(8):1465–1478. doi:10.1007/s10495-007-0076-6

Liu C, Walter TS, Huang P, Zhang S, Zhu X, Wu Y, Wedderburn LR, Tang P, Owens RJ, Stuart DI, Ren J, Gao B (2010) Structural and functional insights of RANKL-RANK interaction and signaling. J Immunol 184(12):6910–6919. doi:10.4049/jimmunol.0904033

Liu C, Zhao Y, He W, Wang W, Chen Y, Zhang S, Ma Y, Gohda J, Ishida T, Walter TS, Owens RJ, Stuart DI, Ren J, Gao B (2015) A RANKL mutant used as an inter-species vaccine for efficient immunotherapy of osteoporosis. Sci Rep 5:14150. doi:10.1038/srep14150

Liu J-L, Zhang J-Z, Lu H-J, Liu B, Si S-Y, Shi S-G, Wu J, Ma Q-J (2009) Construction of *Pichia pastoris* yeast strain with high-efficient expression of HSA-OPG [J]. Bulletin of the Academy of Military Medical Sciences 4:008

Luan X, Lu Q, Jiang Y, Zhang S, Wang Q, Yuan H, Zhao W, Wang J, Wang X (2012) Crystal structure of human RANKL complexed with its decoy receptor osteoprotegerin. J Immunol 189(1):245–252. doi:10.4049/jimmunol.1103387

Miyamoto T (2011) Regulators of osteoclast differentiation and cell-cell fusion. Keio J Med 60(4):101–105

Mizuno A, Amizuka N, Irie K, Murakami A, Fujise N, Kanno T, Sato Y, Nakagawa N, Yasuda H, Mochizuki S, Gomibuchi T, Yano K, Shima N, Washida N, Tsuda E, Morinaga T, Higashio K, Ozawa H (1998) Severe osteoporosis in mice lacking osteoclastogenesis inhibitory factor/osteoprotegerin. Biochem Biophys Res Commun 247(3):610–615

Montanez-Barragan A, Gomez-Barrera I, Sanchez-Nino MD, Ucero AC, Gonzalez-Espinoza L, Ortiz A (2014) Osteoprotegerin and kidney disease. J Nephrol 27(6):607–617. doi:10.1007/s40620-014-0092-x

Morony S, Capparelli C, Lee R, Shimamoto G, Boone T, Lacey DL, Dunstan CR (1999) A chimeric form of osteoprotegerin inhibits hypercalcemia and bone resorption induced by IL-1beta, TNF-alpha, PTH, PTHrP, and 1, 25(OH)2D3. J Bone Miner Res 14(9):1478–1485. doi:10.1359/jbmr.1999.14.9.1478

Nakata S, Yoshida T, Horinaka M, Shiraishi T, Wakada M, Sakai T (2004) Histone deacetylase inhibitors upregulate death receptor 5/TRAIL-R2 and sensitize apoptosis induced by TRAIL/APO2-L in human malignant tumor cells. Oncogene 23(37):6261–6271. doi:10.1038/sj.onc.1207830

Navarre WW, Schneewind O (1994) Proteolytic cleavage and cell wall anchoring at the LPXTG motif of surface proteins in gram-positive bacteria. Mol Microbiol 14(1):115–121

Nelson CA, Warren JT, Wang MW, Teitelbaum SL, Fremont DH (2012) RANKL employs distinct binding modes to engage RANK and the osteoprotegerin decoy receptor. Structure 20(11):1971–1982. doi:10.1016/j.str.2012.08.030

Neville-Webbe HL, Cross NA, Eaton CL, Nyambo R, Evans CA, Coleman RE, Holen I (2004) Osteoprotegerin (OPG) produced by bone marrow stromal cells protects breast cancer cells from TRAIL-induced apoptosis. Breast Cancer Res Treat 86(3):269–279

Nguyen HH, Park J, Kang S, Kim M (2015) Surface plasmon resonance: a versatile technique for biosensor applications. Sensors (Basel) 15(5):10481–10510. doi:10.3390/s150510481

Orita Y, Yamamoto H, Kohno N, Sugihara M, Honda H, Kawamata S, Mito S, Soe NN, Yoshizumi M (2007) Role of osteoprotegerin in arterial calcification: development of new animal model. Arterioscler Thromb Vasc Biol 27(9):2058–2064. doi:10.1161/ATVBAHA.107.147868

Panizo S, Cardus A, Encinas M, Parisi E, Valcheva P, Lopez-Ongil S, Coll B, Fernandez E, Valdivielso JM (2009) RANKL increases vascular smooth muscle cell calcification through a RANK-BMP4-dependent pathway. Circ Res 104(9):1041–1048. doi:10.1161/CIRCRESAHA.108.189001

Polek TC, Talpaz M, Darnay BG, Spivak-Kroizman T (2003) TWEAK mediates signal transduction and differentiation of RAW264.7 cells in the absence of Fn14/TweakR. Evidence for a second TWEAK receptor. J Biol Chem 278(34):32317–32323. doi:10.1074/jbc.M302518200

Pritzker LB, Scatena M, Giachelli CM (2004) The role of osteoprotegerin and tumor necrosis factor-related apoptosis-inducing ligand in human microvascular endothelial cell survival. Mol Biol Cell 15(6):2834–2841. doi:10.1091/mbc.E04-01-0059

Rachner TD, Benad P, Rauner M, Goettsch C, Singh SK, Schoppet M, Hofbauer LC (2009) Osteoprotegerin production by breast cancer cells is suppressed by dexamethasone and confers resistance against TRAIL-induced apoptosis. J Cell Biochem 108(1):106–116. doi:10.1002/jcb.22232

Sattler AM, Schoppet M, Schaefer JR, Hofbauer LC (2004) Novel aspects on RANK ligand and osteoprotegerin in osteoporosis and vascular disease. Calcif Tissue Int 74(1):103–106. doi:10.1007/s00223-003-0011-y

Secchiero P, Corallini F, Beltrami AP, Ceconi C, Bonasia V, Di Chiara A, Ferrari R, Zauli G (2010) An imbalanced OPG/TRAIL ratio is associated to severe acute myocardial infarction. Atherosclerosis 210(1):274–277. doi:10.1016/j.atherosclerosis.2009.11.005

Shipman CM, Croucher PI (2003) Osteoprotegerin is a soluble decoy receptor for tumor necrosis factor-related apoptosis-inducing ligand/Apo2 ligand and can function as a paracrine survival factor for human myeloma cells. Cancer Res 63(5):912–916

Simonet WS, Lacey DL, Dunstan CR, Kelley M, Chang MS, Luthy R, Nguyen HQ, Wooden S, Bennett L, Boone T, Shimamoto G, DeRose M, Elliott R, Colombero A, Tan HL, Trail G, Sullivan J, Davy E, Bucay N, Renshaw-Gegg L, Hughes TM, Hill D, Pattison W, Campbell P, Sander S, Van G, Tarpley J, Derby P, Lee R, Boyle WJ (1997) Osteoprotegerin: a novel secreted protein involved in the regulation of bone density. Cell 89(2):309–319

Theill LE, Boyle WJ, Penninger JM (2002) RANK-L and RANK: T cells, bone loss, and mammalian evolution. Annu Rev Immunol 20:795–823. doi:10.1146/annurev.immunol.20.100301.064753

Truneh A, Sharma S, Silverman C, Khandekar S, Reddy MP, Deen KC, McLaughlin MM, Srinivasula SM, Livi GP, Marshall LA, Alnemri ES, Williams WV, Doyle ML (2000) Temperature-sensitive differential affinity of TRAIL for its receptors. DR5 is the highest affinity receptor. J Biol Chem 275(30):23319–23325. doi:10.1074/jbc.M910438199

Vaccarezza M, Bortul R, Fadda R, Zweyer M (2007) Increased OPG expression and impaired OPG/TRAIL ratio in the aorta of diabetic rats. Med Chem 3(4):387–391

Vitovski S, Phillips JS, Sayers J, Croucher PI (2007) Investigating the interaction between osteoprotegerin and receptor activator of NF-kappaB or tumor necrosis factor-related apoptosis-inducing ligand: evidence for a pivotal role for osteoprotegerin in regulating two distinct pathways. J Biol Chem 282(43):31601–31609. doi:10.1074/jbc.M706078200

Wada T, Nakashima T, Hiroshi N, Penninger JM (2006) RANKL-RANK signaling in osteoclastogenesis and bone disease. Trends Mol Med 12(1):17–25. doi:10.1016/j.molmed.2005.11.007

Walczak H, Miller RE, Ariail K, Gliniak B, Griffith TS, Kubin M, Chin W, Jones J, Woodward A, Le T, Smith C, Smolak P, Goodwin RG, Rauch CT, Schuh JC, Lynch DH (1999) Tumoricidal activity of tumor necrosis factor-related apoptosis-inducing ligand in vivo. Nat Med 5(2):157–163. doi:10.1038/5517

Yamaguchi K, Kinosaki M, Goto M, Kobayashi F, Tsuda E, Morinaga T, Higashio K (1998) Characterization of structural domains of human osteoclastogenesis inhibitory factor. J Biol Chem 273(9):5117–5123

Zhang S, Liu C, Huang P, Zhou S, Ren J, Kitamura Y, Tang P, Bi Z, Gao B (2009) The affinity of human RANK binding to its ligand RANKL. Arch Biochem Biophys 487(1):49–53. doi:10.1016/j.abb.2009.04.008

Zhao Y, Jin M, Ma J, Zhang S, Li W, Chen Y, Zhou Y, Tao H, Liu Y, Wang L, Han H, Niu G, Tao H, Liu C, Gao B (2013) Inhibition effect of enteropeptidase on RANKL-RANK signalling by cleavage of RANK. FEBS Lett 587(18):2958–2964. doi:10.1016/j.febslet.2013.08.005